

Thermopower and the Mott formula for a Majorana edge state

Chang-Yu Hou,^{1,2} Kirill Shtengel,^{1,3} and Gil Refael²

¹*Department of Physics and Astronomy, University of California at Riverside, Riverside, CA 92521*

²*Department of Physics, California Institute of Technology, Pasadena, CA 91125*

³*Institute for Quantum Information, California Institute of Technology, Pasadena, CA 91125*

(Dated: August 9, 2013)

We study the thermoelectric effect between a conducting lead and a Majorana edge state. In the tunneling limit, we first use the Landauer-Büttiker formalism to derive the Mott formula relating the thermopower and the differential conductance between a conducting lead and a superconductor. When the tunneling takes place between a conducting lead and a Majorana edge state, we show that a non-vanishing thermopower can exist. Combining measurements of the differential conductance and the voltage induced by the temperature difference between the conducting lead and the edge state, the Mott formula provides a unique way to infer the temperature of the Majorana edge state.

PACS numbers:

I. INTRODUCTION

Electron thermometry is a crucial component in most condensed matter experiments. It is especially necessary for exploring the unconventional thermoelectric response of low-dimensional systems^{1,2}. One technique for probing the electron temperature utilizes the Seebeck effect by measuring the thermally induced voltage difference between a sample and a weakly coupled lead in the absence of a current. Then, using the Mott formula³⁻⁵,

$$\mathcal{S} = -\frac{\Delta V}{\Delta T} = \frac{\pi^2}{3} \left(\frac{k_B^2 T}{e} \right) \left(\frac{d \ln G(E)}{dE} \right)_{E=\mu}, \quad (1.1)$$

the temperature of the sample can be inferred from the differential conductance, $G(E)$, at energy E . Here, \mathcal{S} is the thermopower (Seebeck coefficient) defined as the ratio of the voltage difference, ΔV , and the temperature difference, ΔT , between the sample and the lead, while T and μ can be taken as the average temperature and chemical potential, respectively. Experimentally, such a technique was first demonstrated in quantum point-contact devices^{6,7} and later used to measure the temperature variation of quantum Hall edge states⁸.

In this paper, we consider thermal and electric transport between a conducting lead and a Majorana edge state that appears at the boundary of a two-dimensional chiral p -wave superconductor⁹. It is not clear, a priori, whether a non-vanishing thermopower can be established, since the Majorana edge mode is charge-neutral due to its underlying particle-hole symmetry. Here, we use the Landauer-Büttiker formalism¹⁰⁻¹⁴ and show that the Mott formula for the thermopower between a superconducting sample and a conducting lead is satisfied in general once both normal and Andreev scattering processes are taken into account.¹⁵ We will then focus on several simplified models in order to address the utility of the Mott formula for probing the temperature of a Majorana edge state. This technique could be naturally used in p + ip superconductors to probe the non-Abelian nature of Majorana zero modes through their unique magneto-thermoelectric signatures¹⁶.

The paper is organized as follows. In Sec. II, we consider

a setup in which a quantum dot with discrete quantum levels couples weakly to a Majorana edge state. As a proof of principle, we show that the thermoelectric response in such setups can be non-vanishing. In the absence of a current, a finite voltage is established in the presence of a temperature difference between the quantum dot and the edge state. In Sec. III, the linear thermoelectric response coefficients between a metallic and a superconducting lead are expressed in terms of scattering probabilities within the framework of the Landauer-Büttiker formalism. The Mott formula is then derived from the response coefficients. In Sec. IV, we explicitly derive the scattering matrix for a single-channel lead coupled to a Majorana edge state. Two scenarios are considered: (a) a single point-contact and (b) a double point-contact. We demonstrate that the single point-contact setup has vanishing thermopower, while the double point-contact setup generically has non-vanishing thermopower. We also discuss the possible thermopower strength for case (b). We conclude our paper in Sec. V. To supplement discussions in the main text, we also include two Appendices that provide a proof of the Onsager relation and a list of the scattering matrix elements for a double-point-contact setup.

II. COUPLING BETWEEN A QUANTUM DOT AND THE MAJORANA EDGE STATE

To gain some intuition as to how a non-vanishing thermopower can arise between a conducting lead and the Majorana edge state, we begin by considering a simplified model in which a conducting lead is replaced by a non-superconducting quantum dot, as schematically shown in Fig. 1.

A. Single-state quantum dot

Let us first consider the case in which a quantum dot consisting of a single quantum state weakly couples to the chiral Majorana edge state as shown in Fig. 1a. The quantum dot has temperature T_n and chemical potential μ_n , while the chiral Majorana edge state has temperature T_s and chemical poten-

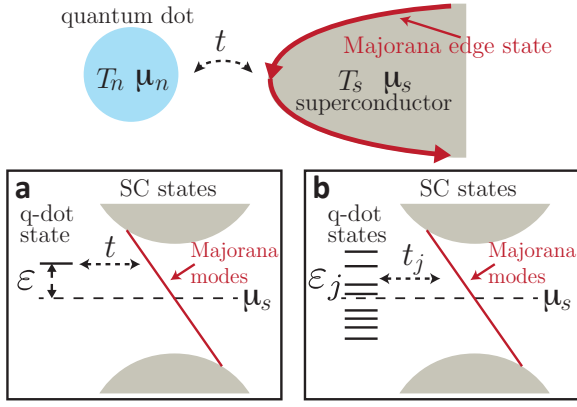


FIG. 1: The upper panel schematically depicts a quantum dot weakly coupling to a Majorana edge state. The temperature and chemical potential of the quantum dot are T_n and μ_n , respectively, and those of the Majorana edge state are T_s and μ_s . (a) A quantum dot with a single energy level ε is coupled to a Majorana edge state with tunneling strength t . (b) Multiple energy levels ε_j of a quantum dot are coupled to a Majorana edge state with tunneling strengths t_j for each state.

tial $\mu_s = 0$. All energies are measured with respect to the chemical potential of the superconductor.

In the continuum limit, the effective Hamiltonian reads

$$H = \varepsilon c^\dagger c + i \frac{v_m}{2} \int \eta(x) \partial_x \eta(x) dx + it(c + c^\dagger) \eta(0) \quad (2.1)$$

where c is the annihilation operator of the fermionic state with energy ε in the quantum dot¹⁷, $\eta(x)$ represents the chiral Majorana fermion mode^{9,18}, v_m is the velocity of the edge state, and the coordinate x runs along the boundary of the superconductor.¹⁹ The last term describes the fermionic coupling, with strength t , between the quantum dot and the Majorana edge state at $x = 0$. The Majorana edge state appears at the boundary of a two-dimensional chiral p -wave superconductor, which reflects the topological property of the superconductor⁹. As a result of the spontaneously broken time-reversal symmetry, it flows with a definite chirality along the edge, akin to the quantum Hall edge state. However, since the Majorana edge state is Bogoliubov-de Gennes quasiparticles, it consists of half of the quantum Hall edge state degrees of freedom. Due to the particle-hole symmetry, the Majorana edge state is formally expressed as a chiral real (Majorana) field, $\eta(x)$.

The Majorana edge state can be represented in momentum space by

$$\eta(x) = \int_{-\infty}^{\infty} \frac{dk}{2\pi} e^{-ikx} \eta(k), \quad (2.2)$$

where $\eta^\dagger(k) = \eta(-k)$ due to the real nature of the field, $\eta^\dagger(x) = \eta(x)$. Under the transformation, we have

$$H = \varepsilon c^\dagger c + \int_{k>0} \frac{dk}{2\pi} \varepsilon_k \eta^\dagger(k) \eta(k) + it(c + c^\dagger) \int_{k>0} \frac{dk}{2\pi} (\eta(k) + \eta^\dagger(k)), \quad (2.3)$$

where the spectrum of the edge state is given by $\varepsilon_k = v_m k$ and we have used the relation $\eta^\dagger(k) = \eta(-k)$ for the last term. Note that the symbol ε is used to denote the energy spectrum of either the quantum dot or the edge modes. Now, we can treat the first line of Eq. (2.3) as the unperturbed Hamiltonian H_0 , and the second line as the perturbed term V .

The transition rate between the quantum dot and the edge state is given by the Fermi-golden rule,

$$T(i \rightarrow f) = \frac{2\pi}{\hbar} |\langle f|V|i \rangle|^2 \delta(E_i - E_f), \quad (2.4)$$

where i and f indicate the initial and the final states of a tunneling process with the corresponding total energies E_i and E_f of the system, respectively, and the delta function enforces the energy conservation. To compute the matrix elements, let us denote the states of the system as $|n_c n_{\eta(k)}\rangle$, where $n_c, n_{\eta(k)} = 0, 1$ represent occupation numbers of the quantum dot state and chiral edge states with energy ε_k respectively. With the assumption $\varepsilon > 0$, energy conservation implies that fermions can tunnel between states with energy $\varepsilon_k = \varepsilon$ for single particle processes. Only two matrix elements $\langle 01|V|10 \rangle = \langle 10|V|01 \rangle = it$ are non-vanishing and give tunneling rates

$$T(10 \rightarrow 01) = T(01 \rightarrow 10) = \frac{2\pi}{\hbar} t^2 \delta(\varepsilon - \varepsilon_k). \quad (2.5)$$

With these tunneling rate, the current tunneling from the quantum dot to the edge state can be written as

$$I = -\frac{e}{\hbar} \frac{t^2}{v_m} [f_n(\varepsilon) - f_s(\varepsilon)], \quad (2.6)$$

where $f_n(E)$ and $f_s(E)$ are the Fermi-Dirac distributions of the quantum dot and the edge state, respectively. To first order in $\mu_n - \mu_s$ and $T_n - T_s$, we obtain a linearized current response

$$I = \frac{e}{\hbar} \frac{t^2}{v_m} \left(\frac{\partial f_s(E)}{\partial E} \right)_{E=\varepsilon} \left[(\mu_n - \mu_s) + \frac{\varepsilon}{T_s} (T_n - T_s) \right], \quad (2.7)$$

that generically has a thermoelectric response such that the temperature difference will lead to a potential difference with a vanishing current and hence a non-vanishing thermopower.

B. Multilevel quantum dot

For a quantum dot whose energy spectrum contains multiple levels as shown in Fig. 1b, the Hamiltonian can be modeled as $\sum_j \varepsilon_j c_j^\dagger c_j$, where c_j is the annihilation operator for the state with energy ε_j . Now, the Hamiltonian representing the coupling between the quantum dot states and the Majorana edge state can be generically written as

$$V = +i \sum_j t(\varepsilon_j) (c_j + c_j^\dagger) \int_{k>0} (\eta(k) + \eta^\dagger(k)), \quad (2.8)$$

where $t(\varepsilon_j)$ is the coupling strength for each energy ε_j .

In the weak tunneling limit, i.e., where higher order scattering processes are neglected, the linearized current flowing from the quantum dot to the edge state becomes

$$I = \frac{e}{\hbar} \sum_j \frac{t(\varepsilon_j)^2}{v_m} \left(\frac{\partial f_s(E)}{\partial E} \right)_{E=\varepsilon_j} \left[(\mu_n - \mu_s) + \frac{\varepsilon_j}{T_s} (T_n - T_s) \right]. \quad (2.9)$$

Now, a finite thermoelectric response appears when the summation of the second term is finite. In the continuum limit, we can define the density of states of the quantum dot as $\rho(E)$ and take $\varepsilon_j \rightarrow E$ to the continuum energy. Because $E(\partial f(E)/\partial E)$ is an odd function of energy E , we need $\rho(E)t(E)^2$ to be non-even in order for the thermopower not to vanish. Hence we conclude that the asymmetry of $\rho(E)t(E)^2$ as a function of energy is crucial for obtaining a finite thermopower.

Since only lowest-order tunneling processes are considered throughout this section, we have neglected higher-order scattering processes present at NS junctions, specifically Andreev scattering. To include contributions of Andreev scattering processes, we will employ the Landauer–Büttiker formalism for scattering between the conducting lead and the superconductor in the next section.

III. LANDAUER–BÜTTIKER SCATTERING FORMALISM

As we have shown in the previous section, the thermopower at the boundary between a quantum dot and a Majorana edge state is generically non-vanishing. Here, by using the Landauer–Büttiker formula, we derive a Mott formula for the thermopower between a conducting lead and a superconducting region, akin to the normal Mott formula in Eq. (1.1).

Let us consider a generic setup shown in Fig. 2, in which a conducting lead weakly couples to a superconductor lead. The temperature and chemical potential of the conducting lead are T_n and μ_n , respectively, and those of the superconductor are T_s and μ_s . Again, we set $\mu_s = 0$ in what follows. To adapt the Landauer–Büttiker formula, we describe both the conducting lead and the superconductor by one-dimensional channels. Since a quasiparticle can scatter into either a quasiparticle or a quasihole, we need to specify numbers of quasiparticle (p) and quasihole (h) channels. At a given energy E , we denote $N_{n\alpha}(E)$ and $N_{s\alpha}(E)$ as the number of $\alpha = p/h$ channels of the conducting lead and the superconductor, respectively. We note that quasiparticles are electrons in the conducting lead while in the superconductor they are Bogolyubov–de Gennes quasiparticles.

In the weak tunneling and dc limits, all transport properties between the conducting lead and the superconductor are governed by a unitary scattering matrix. The scattering matrix elements, which give scattering amplitudes from channel (j, β, b) to (ℓ, α, a) , are denoted by $s_{j\beta b}^{\ell\alpha a}(E)$. Here, $\ell, j = n/s$ are lead indices, $\alpha, \beta = p/h$ are particle/hole indices, and $a = 1, \dots, N_{\ell\alpha}(E)$ ($b = 1, \dots, N_{j\beta}(E)$) are channel indices. We adopt the convention that lower indices represent an incoming state while the upper indices represent an outgoing state. The

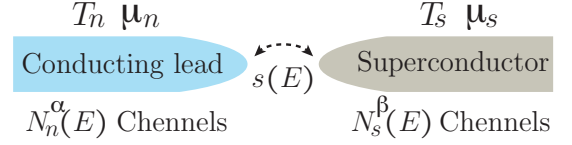


FIG. 2: Schematic picture of a tunneling junction between a conducting lead and a superconductor. The conducting lead has $N_n^\alpha(E)$ channels at energy E while the superconductor has $N_s^\beta(E)$, where $\alpha(\beta) = p, h$ represents the quasiparticle or quasihole channels. The temperature and chemical potential of the conducting lead are T_n and μ_n respectively, and those of the superconductor are T_s and μ_s . $s(E)$ represents the scattering matrix across the tunneling junction.

particle–hole symmetry of superconductors gives

$$s_{j\beta b}^{\ell\alpha a}(E) = \alpha\beta [s_{j\beta b}^{\ell\bar{\alpha}\bar{a}}(-E)]^*, \quad (3.1)$$

where particle indices $\alpha, \beta = p/h$ are defined as $+/-$ in the equation and $\bar{\alpha}, \bar{\beta}$ are defined as $\bar{p}, \bar{h} \equiv h, p$.

Now, the probability of an incoming current at the channel (j, β, b) scattering into the outgoing current at the channel (ℓ, α, a) is given by $|s_{j\beta b}^{\ell\alpha a}(E)|^2$. As we are interested in the total tunneling current between the conducting lead and the superconductor, it is convenient to trace out channel indices and introduce the scattering probability

$$P_{j\beta}^{\ell\alpha}(E) = \sum_{a,b} |s_{j\beta b}^{\ell\alpha a}(E)|^2 \quad (3.2)$$

for the current in the (j, β) state to scatter into the (ℓ, α) state. Here, $\ell = j$ corresponds to reflection while $\ell \neq j$ correspond to transmission. The processes with $\alpha \neq \beta$ are Andreev scattering processes. Due to the unitarity of the scattering matrix, scattering probabilities satisfy

$$\sum_{j\beta} P_{j\beta}^{\ell\alpha}(E) = N_{i\alpha}(E), \quad \sum_{\ell\alpha} P_{j\beta}^{\ell\alpha}(E) = N_{j\beta}(E). \quad (3.3)$$

The particle–hole symmetry, Eq. (3.1), further implies that

$$P_{j\beta}^{\ell\bar{\alpha}}(-E) = P_{j\beta}^{\ell\alpha}(E). \quad (3.4)$$

Combining Eqs. (3.3) and (3.4), we find that the number of channels satisfies $N_{\ell h}(E) = N_{\ell p}(-E)$.

Now, electric and heat currents can be expressed in terms of scattering probabilities^{12–14}. The electric current reads

$$I = \frac{e}{\hbar} \int_0^\infty dE \left\{ -f_n^p(E) (N_{np} - P_{np}^{np} + P_{np}^{nh}) + f_n^h(E) (N_{nh} - P_{nh}^{nh} + P_{nh}^{np}) + f_s^p(E) (P_{sp}^{np} - P_{sp}^{nh}) + f_s^h(E) (P_{sh}^{nh} - P_{sh}^{np}) \right\}, \quad (3.5)$$

while the heat current reads

$$Q = \frac{1}{\hbar} \int_0^\infty dE E \left\{ +f_n^p(E) (N_{np} - P_{np}^{np} - P_{np}^{nh}) + f_n^h(E) (N_{nh} - P_{nh}^{nh} - P_{nh}^{np}) - f_s^p(E) (P_{sp}^{np} + P_{sp}^{nh}) - f_s^h(E) (P_{sh}^{np} + P_{sh}^{nh}) \right\}, \quad (3.6)$$

where energy dependences of all $N_{\ell\alpha}$ and $P_{j\beta}^{\ell\alpha}$ are implied. The Fermi-Dirac distributions of particles and holes are given by

$$f_{\ell}^{\alpha}(E) = (e^{(E \pm \mu_{\ell})/k_B T_{\ell}} + 1)^{-1}, \quad (3.7)$$

where $\ell = n/s$ and $\alpha = p/h$. The “+” sign in the exponent corresponds to particles ($\alpha = p$), the “-” sign – to holes ($\alpha = h$). Since the particle–hole picture effectively maps quasiparticles with negative energy to quasiholes with positive energy, the integration in Eqs. (3.5) and (3.6) is performed only over the positive energy region to avoid double counting. Intuitively, the expression of the electric current in Eq. (3.5) sums over flows in all channels of the conducting lead multiplied by the sign of their charge carriers (negative(positive) charge for the electron(hole)) while the heat flow expression in Eq. (3.6) sums over energy flows in all channels.

With the aid of the unitarity properties (3.3) and the particle–hole symmetry (3.4), the electric current becomes

$$I = \frac{-e}{h} \int_{-\infty}^{\infty} dE (f_n^p - f_s^p) (N_{np} - P_{np}^{np} + P_{np}^{nh}), \quad (3.8)$$

while the heat current can be rewritten as

$$Q = \frac{1}{h} \int_{-\infty}^{\infty} dE E (f_n^p - f_s^p) (N_{np} - P_{np}^{np} - P_{np}^{nh}). \quad (3.9)$$

Here, we have used the relation $f_n^h(E) = 1 - f_n^p(-E)$ to extend the range of integration to all energies. Importantly, both electric and heat currents involve only reflection probabilities in the conducting leads.¹²

To linear order, the expressions for the electric and heat currents can be organized in terms of the chemical potential difference $\Delta\mu = \mu_n - \mu_s$ and the temperature difference $\Delta T = T_n - T_s$ as

$$\begin{pmatrix} I/(-e) \\ Q \end{pmatrix} = \begin{pmatrix} L_{11} & L_{12}/T_s \\ L_{21} & L_{22}/T_s \end{pmatrix} \begin{pmatrix} \Delta\mu \\ \Delta T \end{pmatrix}. \quad (3.10)$$

The linear response coefficients L_{ij} are given by

$$L_{11} = \frac{-1}{h} \int_{-\infty}^{\infty} dE \frac{\partial f}{\partial E} (N_{np} - P_{np}^{np} + P_{np}^{nh}), \quad (3.11a)$$

$$L_{12} = \frac{-1}{h} \int_{-\infty}^{\infty} dE E \frac{\partial f}{\partial E} (N_{np} - P_{np}^{np} + P_{np}^{nh}), \quad (3.11b)$$

$$L_{21} = \frac{-1}{h} \int_{-\infty}^{\infty} dE E \frac{\partial f}{\partial E} (N_{np} - P_{np}^{np} - P_{np}^{nh}), \quad (3.11c)$$

$$L_{22} = \frac{-1}{h} \int_{-\infty}^{\infty} dE E^2 \frac{\partial f}{\partial E} (N_{np} - P_{np}^{np} - P_{np}^{nh}). \quad (3.11d)$$

As shown in Appendix A, the Onsager reciprocal relation is satisfied for these linear response coefficients. In the presence of time-reversal symmetry, one can show that $L_{12} = L_{21}$ even though the expressions given by Eqs. (3.11) do not directly reflect this. In the absence of time-reversal symmetry, linear-response coefficients between the system and its time-reversed system are related due to the Onsager relation, i.e., $L_{12} = \mathcal{T}[L_{21}]$, where $\mathcal{T}[\dots]$ represents the coefficient in the time-reversed system.

As we are interested in the relation between L_{11} and L_{12} , it is convenient to define a function

$$K(E) = N_{np}(E) - P_{np}^{np}(E) + P_{np}^{nh}(E). \quad (3.12)$$

When the tunneling probabilities are smooth functions of energy E , the linear response coefficients L_{ij} can be approximated by Sommerfeld expansions.²⁰ To the lowest non-vanishing order, the Sommerfeld expansion of L_{11} is given by

$$L_{11} \approx \frac{1}{h} K(E) \Big|_{E=0} + O(k_B T_s)^2, \quad (3.13)$$

while the Sommerfeld expansion of L_{12} reads

$$L_{12} \approx \frac{1}{h} \frac{\pi^2}{3} (k_B T_s)^2 \frac{dK(E)}{dE} \Big|_{E=0} + O(k_B T_s)^4. \quad (3.14)$$

We observe that both L_{11} and L_{12} can be related to the differential conductance by $G(E = eV) = -\frac{e^2}{h} K(E)$ with an applied voltage V at the normal lead and with a fixed chemical potential at the superconductor.

Now, the thermopower (Seebeck coefficient) can be readily evaluated and shown to satisfy the Mott formula

$$S = -\frac{\Delta V}{\Delta T} = \frac{1}{e T_s} \frac{L_{12}}{L_{11}} = \frac{\pi^2}{3} \frac{k_B^2 T_s}{e} \frac{d \ln G(E)}{dE} \Big|_{E=\mu_s}. \quad (3.15)$$

Here, ΔV is the voltage in response to the temperature difference ΔT between the tunneling junction in the absence of total current. The thermopower vanishes when the differential conductance is an even function of energy E . The presence of the Mott relation provides a unique way to infer the temperature difference by measuring the differential conductance and the voltage difference between the conducting lead and the superconductor.

IV. SINGLE-CHANNEL CONTINUUM MODELS

In this section, we discuss two simplified models that describe a single-channel conducting lead tunneling into a chiral Majorana edge state. These models provide examples in which the thermopower is (A) vanishing as tunneling probabilities have no energy dependence due to an accidental symmetry for a single-point contact setup, or (B) non-vanishing as tunneling probabilities gain energy dependence in a double-points contact setup. The goal here is not to present realistic models for such systems, but rather to argue that the scenario (B) represents a generic case for a realistic system.

A. Single-point-contact geometry

Let us consider a setup where a tip of a single-channel conducting lead couples to a chiral Majorana edge state. In such a case, the non-chiral channel can be unfolded to form a chiral

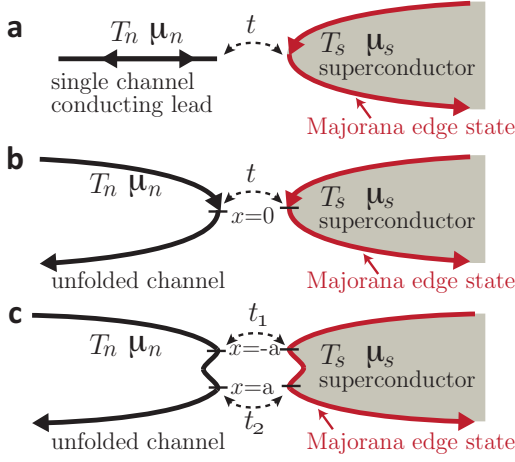


FIG. 3: (a) Schematic plot of a tip of a single-channel lead coupled to a Majorana edge state (red curve at the boundary of the superconductor). The tunneling strength is t . The temperature and chemical potential of the conducting lead are T_n and μ_n , respectively, and those of the Majorana edge state are T_s and μ_s . (b) A single-electron channel can be unfolded into a chiral electron channel that couples to a Majorana edge state at the point $x = 0$. (c) The plot shows a toy model of a double-point-contact setup between an unfolded electronic channel and a Majorana edge state. Two tunneling points are at $x = \pm a$ along the chiral electron mode.

electron mode as depicted in Fig. 3b. The coupling Hamiltonian is given by^{18,21}

$$\begin{aligned}
 H &= H_N + H_{MF} + H_t, \\
 H_N &= -iv_f \int_{-\infty}^{\infty} dx \psi^\dagger(x) \partial_x \psi(x), \\
 H_{MF} &= -i \frac{v_m}{2} \int_{-\infty}^{\infty} dx \eta(x) \partial_x \eta(x), \\
 H_t &= \frac{i}{\sqrt{2}} \int_{-\infty}^{\infty} dx \left(t \psi(x) + t^* \psi^\dagger(x) \right) \eta(x) \delta(x).
 \end{aligned} \tag{4.1}$$

Here, the $\psi(x)$ is the annihilation operators for the chiral electron mode with velocity v_f , $\eta(x)$ is the chiral Majorana mode with velocity v_m , and t is the coupling strength. ψ satisfies the usual fermionic commutation relations, while the Majorana fermion satisfying the anticommutation relation $\{\eta(x), \eta(x')\} = \delta(x - x')$. The equations of motion are readily written as

$$\partial_t \psi = -v_f \partial_x \psi + t^* \eta \delta(x) / \sqrt{2}, \tag{4.2}$$

$$\partial_t \psi^\dagger = -v_f \partial_x \psi^\dagger + t \eta \delta(x) / \sqrt{2}, \tag{4.3}$$

$$\partial_t \eta = -v_m \partial_x \eta - (t \psi + t^* \psi^\dagger) \delta(x) / \sqrt{2}. \tag{4.4}$$

By removing the time dependence with the Ansatz

$$\psi = e^{-iEt} \psi(x), \quad \psi^\dagger = e^{-iEt} \psi^\dagger(x), \quad \eta = e^{-iEt} \eta(x), \tag{4.5}$$

we have

$$\begin{aligned}
 v_f \partial_x \psi(x) &= iE \psi(x) + t^* \eta(x) \delta(x) / \sqrt{2}, \\
 v_f \partial_x \psi^\dagger(x) &= iE \psi^\dagger(x) + t \eta(x) \delta(x) / \sqrt{2}, \\
 v_m \partial_x \eta(x) &= iE \eta(x) - (t \psi(x) + t^* \psi^\dagger(x)) \delta(x) / \sqrt{2}.
 \end{aligned} \tag{4.6}$$

Now, a single-point-contact scattering problem at $x = 0$ can be solved by the transfer matrix method. First, the delta function $\delta(x)$ is approximated as a bump function with width ℓ and height $1/\ell$. Then, the transfer matrix of this bump geometry can be obtained by partitioning the width ℓ by $N \rightarrow \infty$ steps. Finally, the $\delta(x)$ function is recovered by taking the limit $\ell \rightarrow 0$. By following these steps, we connect operators at $x = 0^+$ to operators at $x = 0^-$ by a transfer matrix M as

$$\begin{pmatrix} \eta(0^+) \\ \psi(0^+) \\ \psi^\dagger(0^+) \end{pmatrix} = M \begin{pmatrix} \eta(0^-) \\ \psi(0^-) \\ \psi^\dagger(0^-) \end{pmatrix}. \tag{4.7}$$

As this transfer matrix M gives the particle hopping amplitudes but not the current scattering amplitudes between the conducting lead and the Majorana edge state, it is convenient to convert the transfer matrix to the scattering matrix associating with the current scattering by including the effect of different velocities. We obtain the scattering matrix

$$\begin{aligned}
 S^t &= \begin{pmatrix} s_\eta^\eta & s_p^\eta & s_h^\eta \\ s_\eta^p & s_p^p & s_h^p \\ s_\eta^h & s_p^h & s_h^h \end{pmatrix} \\
 &= \begin{pmatrix} \cos 2|\tilde{t}| & -\frac{e^{i\phi}}{\sqrt{2}} \sin 2|\tilde{t}| & -\frac{e^{-i\phi}}{\sqrt{2}} \sin 2|\tilde{t}| \\ \frac{e^{-i\phi}}{\sqrt{2}} \sin 2|\tilde{t}| & \cos^2 |\tilde{t}| & -e^{-2i\phi} \sin^2 |\tilde{t}| \\ \frac{e^{i\phi}}{\sqrt{2}} \sin 2|\tilde{t}| & -e^{2i\phi} \sin^2 |\tilde{t}| & \cos^2 |\tilde{t}| \end{pmatrix},
 \end{aligned} \tag{4.8}$$

where the effective coupling constant \tilde{t} is defined as $\tilde{t} = t / (2\sqrt{v_f v_m})$ with ϕ being its phase: $t = |\tilde{t}| e^{i\phi}$. The s_β^α are matrix elements corresponding to scattering amplitudes of a quasiparticle type β scattering to type α . Here, η , p and h indicate Majorana edge mode, electron and hole. One can directly verify that this scattering matrix S is unitary.

From Eq. (3.2), we conclude that the scattering probabilities have no energy and phase dependence. Thereby, the kernel defined in Eq. (3.12) and, consequently, the differential conductance will not depend on the energy of the incoming flows. It then follows from the Mott relation (3.15) that the thermopower vanishes for the single-point-contact geometry. This is a consequence of uniform coupling strengths between the states with different energies along with the constant density of states of both electronic and Majorana modes – an artifact of our model.

B. Double-point-contact geometry

To emulate the finite extent of the tunneling region between a conducting lead and a Majorana edge state, we consider a double-point-contact setup. Once again, for simplicity, the non-chiral channel in the conducting lead is unfolded to form a chiral electronic mode. With two point contacts at $x = \pm a/2$, as shown in Fig. 3(c), the tunneling Hamiltonian H_t becomes

$$\begin{aligned}
 H_t &= \frac{i}{\sqrt{2}} \left(t_1 \psi(-a/2) + t_1^* \psi^\dagger(-a/2) \right) \eta(-a/2) \\
 &\quad + \frac{i}{\sqrt{2}} \left(t_2 \psi(a/2) + t_2^* \psi^\dagger(a/2) \right) \eta(a/2),
 \end{aligned} \tag{4.9}$$

The scattering matrix S_{tt} which connects currents on both sides of the scattering region can be obtained by combining two scattering matrices in Eq. (4.8) with the transfer matrix, and is given by

$$S'' = S(t_2) \begin{pmatrix} e^{ik_m a} & 0 & 0 \\ 0 & e^{ik_f a} & 0 \\ 0 & 0 & e^{ik_f a} \end{pmatrix} S(t_1). \quad (4.10)$$

Here momenta are defined by $k_f = E/v_f$ and $k_m = E/v_m$ and the tunneling amplitudes are defined by $t_1 = |t_1|e^{i\phi_1}$ and $t_2 = |t_2|e^{i\phi_2}$.

As the full expression of the scattering matrix becomes quite lengthy, we list its elements in Appendix B. Using Eqs. (B1) and (B2), we obtain the kernel defined in Eq. (3.12) as

$$K(E) = 1 - \cos(2|\tilde{t}_1|) \cos(2|\tilde{t}_2|) + \sin(2|\tilde{t}_1|) \sin(2|\tilde{t}_2|) \\ \times \left(\cos^2(|\tilde{t}_1|) \cos(\tilde{k}a - \phi_{12}) + \sin^2(|\tilde{t}_1|) \cos(\tilde{k}a + \phi_{12}) \right). \quad (4.11)$$

Here, we have used the notation $\tilde{k} = k_f - k_m$ and $\phi_{12} = \phi_1 - \phi_2$ and defined effective tunneling constants $|\tilde{t}_i| = |t_i|/(2\sqrt{v_f v_m})$, $i = 1, 2$. To have non-vanishing thermopower, $K(E)$ needs to be a non-even function of energy, which requires the phase $\alpha_1 \neq \alpha_2 + n\pi$. Since the phase difference of the contact tunneling strengths can be arbitrary (or tuned by threading magnetic flux), an electric voltage difference will generically appear between the conducting lead and the Majorana edge state. We then expect that a finite tunneling region, in general, leads to a non-vanishing Seebeck coefficient.

We conclude this section by discussing possible signatures of the Seebeck effect in the double-point-contact setup. The purpose is to show that a non-vanishing Seebeck coefficient of reasonable magnitude can appear. In the weak tunneling limit, $|\tilde{t}_1| \sim |\tilde{t}_2| \ll 1$, the energy derivative of the differential conductance can be evaluated from Eq. (4.11), and is given by

$$\left. \frac{d \ln G(E)}{dE} \right|_{E=0} \approx \frac{a}{\hbar} \frac{\sin \phi_{12}}{1 + \cos \phi_{12}} \left(\frac{1}{v_f} - \frac{1}{v_m} \right). \quad (4.12)$$

From the Mott formula in Eq. (3.15), the Seebeck coefficient can be approximated to be

$$S \approx -\frac{\pi^2 k_B^2 T_s}{3} \frac{a}{e \hbar v_m}. \quad (4.13)$$

where we have used $v_m \ll v_f$ as the velocity of the Majorana edge state is reduced by comparison with the Fermi velocity,²² and we have taken the phase-dependent factor, $\sin(\phi_{12})/(1 + \cos(\phi_{12})) \sim 1$, as its median value. For $a \sim 0.1 - 10 \mu\text{m}$ and $v_m \sim 10^4 \text{ m/s}$ at $T_s \sim 100 \text{ mK}$, we expect the value of the thermopower

$$S \sim 10^{-5} - 10^{-3} \text{ V/K}. \quad (4.14)$$

This will result in a reasonably strong signal for the potential difference ΔV when the temperature difference ΔT is around $1 \sim 10 \text{ mK}$. In this limit, we note that the Seebeck coefficient scales linearly with the distance between the two contacts while it is inversely proportional to the propagating velocity of the Majorana edge mode.

V. CONCLUSIONS

In summary, by employing the Landauer-Büttiker formalism, we have demonstrated explicitly that the thermopower (Seebeck coefficient) between a conducting lead and a superconductor satisfies the Mott formula. Using point-contact models, we argued that the thermopower between a conducting lead and a Majorana edge state generically does not vanish. In the absence of current, this leads to a finite voltage when a temperature difference is established across a tunneling junction. With the aid of the Mott formula, the temperature of the Majorana edge state can be inferred by measuring the differential conductance and the voltage across the tunneling region in the absence of current flow. Since this technique has been demonstrated in non-superconducting systems for tunneling geometries⁶⁻⁸, we expect that a similar technique can be used to probe the temperature of Majorana edge states.

Acknowledgments

The authors would like to thank A. R. Akhmerov and D. Pekker for helpful discussions. CYH and KS were supported in part by the DARPA-QuEST program. KS was supported in part by NSF award DMR-0748925. GR is grateful for support from the Packard foundation and the IQIM, an NSF center supported in part by the Moore foundation.

Appendix A: Proof of the Onsager relation

1. Time-reversal-invariant case

From Eq. (3.11), the form of the following linear-response coefficients

$$L_{12} = \frac{1}{h} \int_{-\infty}^{\infty} dE E \left(-\frac{\partial f}{\partial E} \right) (N_{np} - P_{np}^{np} + P_{np}^{nh}), \quad (A1)$$

$$L_{21} = \frac{1}{h} \int_{-\infty}^{\infty} dE E \left(-\frac{\partial f}{\partial E} \right) (N_{np} - P_{np}^{np} - P_{np}^{nh}), \quad (A2)$$

is not identical and does not obviously satisfy the Onsager relation. Our goal here is to show that these linear response coefficients do in fact follow the Onsager reciprocity relation $L_{12} = L_{21}$ in the presence of time reversal symmetry (TRS). We observe that L_{12} and L_{21} differ only by a minus sign in the last term of the integrand. Hence, to satisfy the Onsager relation, the contribution from the last term has to vanish after the integration. In the presence of TRS, we will show that $P_{np}^{nh}(E)$ is indeed an even function of energy and hence does not contribute to the integrals in Eqs. (A1,A2).

Let us define the basis for a scattering problem between a normal and a superconducting lead for spin-1/2 electrons as

$$\left(\psi_{np\uparrow}(E), \psi_{sp\uparrow}(E), \psi_{np\downarrow}(E), \psi_{sp\downarrow}(E), \right. \\ \left. \psi_{nh\uparrow}(E), \psi_{sh\uparrow}(E), \psi_{nh\downarrow}(E), \psi_{sh\downarrow}(E) \right)^T, \quad (A3)$$

where each $\psi_{i\alpha\sigma}(E)$ has $N_{i\alpha\sigma}(E)$ channels that will be indicated by indices a/b in what follows, and σ is the spin index. In this basis, a scattering matrix $S(E)$ has matrix elements

$$S(E) = \left\{ s_{j\beta\sigma'}^{i\alpha\sigma}(E) \right\}_{i,j=n/s;\alpha,\beta=p/h;\sigma,\sigma'=\uparrow,\downarrow} \quad (\text{A4})$$

where each $s_{j\beta\sigma'}^{i\alpha\sigma}$ is an $N_{i\alpha\sigma}(E) \times N_{j\beta\sigma'}(E)$ matrix with its elements denoted by $s_{j\beta\sigma'b}^{i\alpha\sigma a}(E)$, which relates the outgoing current at state $(\ell, \alpha, \sigma', b)$ to the incoming current at state (j, β, σ, a) .

For spin-1/2 electrons, the time reversal transformation of the scattering matrix in the electron basis is given by

$$\mathcal{T}[S] = \sigma_y S^T \sigma_y \quad (\text{A5})$$

where the σ_y is the Pauli matrix acting on spins and the superscript T indicates the transpose of the matrix. With the TRS, we have $\mathcal{T}[S] = S$. (A similar transformation can be defined for spinless electrons by $\mathcal{T}[S] = S^T$. Then all conclusions in this appendix will follow.) For a superconductor, the corresponding time reversal transformation becomes $\mathcal{T}[S] = (\mathbb{1}_{ph} \otimes \sigma_y \otimes \mathbb{1}) S^T (\mathbb{1}_{ph} \otimes \sigma_y \otimes \mathbb{1})$, where the $\mathbb{1}_{ph}$ acts on the particle-hole indices, σ_y acts on the spin indices, and $\mathbb{1}$ acts on the lead-channel indices. The time reversal transformation maps matrix elements of the scattering matrix by

$$\mathcal{T}[S(E)] = \left\{ s_{j\beta\sigma'}^{i\alpha\sigma}(E) \mapsto (\sigma\sigma') \times s_{i\alpha\bar{\sigma}}^{j\beta\bar{\sigma}'}(E)^T \right\} \quad (\text{A6})$$

where $\bar{\sigma}$ and $\bar{\sigma}'$ indicate the flip of spin, i.e., $\bar{\uparrow} = \downarrow$ and vice versa, and the values of σ, σ' inside the parentheses are taken to be ± 1 for $\sigma, \sigma' = \uparrow / \downarrow$.

The presence of TRS implies $S(E) = \mathcal{T}[S(E)]$ and leads to following useful identities for each element

$$\begin{aligned} s_{np\uparrow b}^{nh\uparrow a}(E) &= s_{nh\downarrow a}^{np\downarrow b}(E), & s_{np\downarrow b}^{nh\downarrow a}(E) &= s_{nh\uparrow a}^{np\uparrow b}(E), \\ s_{np\uparrow a}^{nh\uparrow b}(E) &= -s_{nh\downarrow b}^{np\downarrow a}(E), & s_{np\downarrow a}^{nh\downarrow b}(E) &= -s_{nh\uparrow b}^{np\uparrow a}(E). \end{aligned} \quad (\text{A7})$$

Let us recall the definition of the scattering probability $P_{np}^{nh}(E)$ in terms of the scattering matrix elements

$$\begin{aligned} P_{np}^{nh}(E) &= \sum_{\sigma,\sigma';a,b} s_{np\sigma'b}^{nh\sigma a}(E) s_{np\sigma'a}^{nh\sigma b}(E)^* \\ &= - \sum_{\sigma,\sigma';a,b} s_{np\sigma'b}^{nh\sigma a}(E) s_{nh\sigma'a}^{np\sigma b}(-E). \end{aligned} \quad (\text{A8})$$

where we have used the particle-hole symmetry (PHS) given by Eq. (3.1) for the second equality. With the aid of the identities given by Eq. (A7), we have

$$\begin{aligned} P_{np}^{nh}(E) &= \sum_{\sigma,\sigma';a,b} s_{nh\sigma'a}^{np\sigma b}(E) s_{nh\sigma'a}^{np\sigma b}(E)^* \\ &= - \sum_{\sigma,\sigma';a,b} s_{nh\sigma'a}^{np\sigma a}(E) s_{np\sigma'b}^{nh\sigma a}(-E), \end{aligned} \quad (\text{A9})$$

where we again used the PHS for the last equality. Comparing the results in Eqs. (A8) and (A9), we can conclude that $P_{np}^{nh}(E) = P_{np}^{nh}(-E)$. Hence, $P_{np}^{nh}(E)$ is an even function of the energy E and leads to no contribution of the linear response coefficient. Thus, the Onsager reciprocal relation is satisfied in the presence of TRS.

2. Generic case

In the absence of TRS, the Onsager reciprocal relation states that $L_{ij} = \mathcal{T}[L_{ji}]$, where $\mathcal{T}[L_{ji}]$ stands for the linear-response coefficient of the time-reversed system. Therefore we need to verify that the following relations are satisfied

$$L_{11} = \mathcal{T}[L_{11}], \quad L_{22} = \mathcal{T}[L_{22}], \quad L_{12} = \mathcal{T}[L_{21}]. \quad (\text{A10})$$

As Eqs. (3.11) involve one channel number and two tunneling probabilities, $N_{np}(E)$, $P_{np}^{np}(E)$ and $P_{np}^{nh}(E)$, we shall focus on those quantities of the time-reversed system.

First, the number of channels is invariant under the time reversal, i.e., $\mathcal{T}[N_{np}(E)] = N_{np}(E)$. Second, from the definition of the scattering probability $P_{np}^{np}(E) = \sum_{\sigma,\sigma';a,b} |s_{np\sigma'b}^{np\sigma a}|^2$, and time reversed elements in Eq. (A6), $\mathcal{T}[s_{np\sigma'}^{np\sigma}] = (\sigma\sigma') \times s_{np\bar{\sigma}}^{np\bar{\sigma}'}$, we have $\mathcal{T}[P_{np}^{np}(E)] = P_{np}^{np}(E)$ under the time-reversed transformation. Finally, the time reversed form of $\mathcal{T}[P_{np}^{nh}(E)] = \sum_{\sigma,\sigma';a,b} |s_{nh\sigma'a}^{np\sigma b}(E)|^2$, given in Eq. (A9), is not invariant under the time reversal transformation.

We shall now discuss each Onsager relation separately.

a. Diagonal response coefficients

Let us recall the linear response coefficient in Eq. (3.11)

$$L_{11} = \frac{1}{h} \int_{-\infty}^{\infty} dE \left(-\frac{\partial f}{\partial E} \right) (N_{np} - P_{np}^{np} + P_{np}^{nh}). \quad (\text{A11})$$

As both $N_{np}(E)$ and $P_{np}^{np}(E)$ are invariant under the time reversal transformation, we have

$$\begin{aligned} &L_{11} - \mathcal{T}[L_{11}] \\ &= \frac{1}{h} \int dE \left(-\frac{\partial f}{\partial E} \right) (P_{np}^{nh} - \mathcal{T}[P_{np}^{nh}]) \\ &= \frac{1}{h} \int dE \left(-\frac{\partial f}{\partial E} \right) \sum_{\sigma,\sigma';a,b} (|s_{np\sigma'b}^{nh\sigma a}|^2 - |s_{nh\sigma'a}^{np\sigma b}|^2), \quad (\text{A12}) \\ &= \frac{-1}{h} \int_{-\infty}^{\infty} dE \left(-\frac{\partial f}{\partial E} \right) \sum_{\sigma,\sigma';a,b} (s_{np\sigma'b}^{nh\sigma a}(E) s_{nh\sigma'a}^{np\sigma a}(-E) \\ &\quad - s_{nh\sigma'a}^{np\sigma b}(E) s_{np\sigma'a}^{nh\sigma b}(-E)), \end{aligned}$$

where we have used the PHS for the last equality. As all terms inside parentheses are, in overall, odd functions and $(-\frac{\partial f(E)}{\partial E})$ is an even function of energy, the integration vanishes. Hence we have shown that $L_{11} = \mathcal{T}[L_{11}]$. A similar argument shows that $L_{22} = \mathcal{T}[L_{22}]$ as well.

b. *Off-diagonal response coefficients*

From Eqs. (A1) and (A2), we immediately have

$$\begin{aligned}
& L_{12} - \mathcal{T}[L_{21}] \\
&= \frac{1}{h} \int dE E \left(-\frac{\partial f}{\partial E} \right) (P_{np}^{nh} + \mathcal{T}[P_{np}^{nh}]) \\
&= \frac{1}{h} \int dE E \left(-\frac{\partial f}{\partial E} \right) \sum_{\sigma, \sigma', a, b} (|s_{np\sigma' b}^{nh\sigma a}|^2 + |s_{nh\sigma' a}^{np\sigma b}|^2), \quad (\text{A13}) \\
&= - \int_{-\infty}^{\infty} dE E \left(-\frac{\partial f}{\partial E} \right) \sum_{\sigma, \sigma', a, b} (s_{np\sigma' b}^{nh\sigma a}(E) s_{nh\sigma' a}^{np\sigma b}(-E) \\
&\quad + s_{nh\sigma' a}^{np\sigma b}(E) s_{np\sigma' b}^{nh\sigma a}(-E))
\end{aligned}$$

where we have used the PHS for the last equality. Since all terms inside the parentheses are even functions of E while

$E(-\partial f(E)/\partial E)$ is an odd function of energy, the integral vanishes. We therefore obtain $L_{12}^A = \mathcal{T}[L_{21}^A]$.

Appendix B: Scattering matrix elements of two point contact setup

In this Appendix, we list scattering matrix elements s_{β}^{α} of the two-points contact setup. The tunneling amplitudes are defined by $t_1 = |t_1|e^{i\phi_1}$ and $t_2 = |t_2|e^{i\phi_2}$. It is convenient to define effective tunneling amplitudes $|\tilde{t}_i| = |t_i|/(2\sqrt{v_F v_m})$. First, matrix elements associating with the kernel are given by

$$s_p^p = \frac{1}{2} \left(2e^{ik_f a} \left(e^{2i(\phi_1 - \phi_2)} \sin^2(|\tilde{t}_1|) \sin^2(|\tilde{t}_2|) + \cos^2(|\tilde{t}_1|) \cos^2(|\tilde{t}_2|) \right) - e^{i(k_m a + \phi_1 - \phi_2)} \sin(2|\tilde{t}_1|) \sin(2|\tilde{t}_2|) \right), \quad (\text{B1})$$

$$s_p^h = -\frac{1}{2} \left(2e^{ik_f a} \left(e^{2i\phi_1} \sin^2(|\tilde{t}_1|) \cos^2(|\tilde{t}_2|) + e^{2i\phi_2} \cos^2(|\tilde{t}_1|) \sin^2(|\tilde{t}_2|) \right) + e^{i(k_m a + \phi_1 + \phi_2)} \sin(2|\tilde{t}_1|) \sin(2|\tilde{t}_2|) \right). \quad (\text{B2})$$

The rest of the matrix elements are given by

$$s_{\eta}^{\eta} = e^{ik_m a} \cos(2|\tilde{t}_1|) \cos(2|\tilde{t}_2|) - e^{ik_f a} \cos(\phi_1 - \phi_2) \sin(2|\tilde{t}_1|) \sin(2|\tilde{t}_2|) \quad (\text{B3})$$

$$s_p^{\eta} = -\frac{1}{\sqrt{2}} \left(e^{i(k_f a - \phi_2)} \sin(2|\tilde{t}_2|) \left(e^{2i\phi_2} \cos^2(|\tilde{t}_1|) - e^{2i\phi_1} \sin^2(|\tilde{t}_1|) \right) + e^{i(k_m a + \phi_1)} \sin(2|\tilde{t}_1|) \cos(2|\tilde{t}_2|) \right) \quad (\text{B4})$$

$$s_h^{\eta} = -\frac{1}{\sqrt{2}} \left(e^{i(k_f a + \phi_2)} \sin(2|\tilde{t}_2|) \left(e^{-2i\phi_2} \cos^2(|\tilde{t}_2|) - e^{-2i\phi_1} \sin^2(|\tilde{t}_1|) \right) + e^{i(k_m a - \phi_1)} \sin(2|\tilde{t}_1|) \cos(2|\tilde{t}_2|) \right) \quad (\text{B5})$$

$$s_{\eta}^p = \frac{1}{\sqrt{2}} \left(e^{i(k_f a + \phi_1)} \sin(2|\tilde{t}_1|) \left(e^{-2i\phi_1} \cos^2(|\tilde{t}_2|) - e^{-2i\phi_2} \sin^2(|\tilde{t}_2|) \right) + e^{i(k_m a - \phi_2)} \cos(2|\tilde{t}_1|) \sin(2|\tilde{t}_2|) \right) \quad (\text{B6})$$

$$s_h^p = -\frac{1}{2} \left(2e^{ik_f a} \left(e^{-2i\phi_1} \sin^2(|\tilde{t}_1|) \cos^2(|\tilde{t}_2|) + e^{-2i\phi_2} \cos^2(|\tilde{t}_1|) \sin^2(|\tilde{t}_2|) \right) + e^{i(k_m a - \phi_1 - \phi_2)} \sin(2|\tilde{t}_1|) \sin(2|\tilde{t}_2|) \right) \quad (\text{B7})$$

$$s_{\eta}^h = \frac{1}{\sqrt{2}} \left(e^{i(k_f a - \phi_1)} \sin(2|\tilde{t}_1|) \left(e^{2i\phi_1} \cos^2(|\tilde{t}_2|) - e^{2i\phi_2} \sin^2(|\tilde{t}_2|) \right) + e^{i(k_m a + \phi_2)} \cos(2|\tilde{t}_1|) \sin(2|\tilde{t}_2|) \right) \quad (\text{B8})$$

$$s_h^h = \frac{1}{2} \left(2e^{ik_f a} \left(e^{-2i(\phi_1 - \phi_2)} \sin^2(|\tilde{t}_1|) \sin^2(|\tilde{t}_2|) + \cos^2(|\tilde{t}_1|) \cos^2(|\tilde{t}_2|) \right) - e^{i(k_m a - \phi_1 + \phi_2)} \sin(2|\tilde{t}_1|) \sin(2|\tilde{t}_2|) \right) \quad (\text{B9})$$

With these matrix elements, one can show that the scattering matrix $S''(\mathcal{E})$ is unitary and satisfies the particle-hole symme-

try defined in Eq. (3.1).

¹ C. L. Kane and M. P. A. Fisher, Phys. Rev. Lett. **76**, 3192 (1996).

² C. L. Kane and M. P. A. Fisher, Phys. Rev. B **55**, 15832 (1997).

³ N. F. Mott and H. Jones, *The Theory of the Properties of Metals and Alloys* (Dover Publications, New York, 1958).

⁴ M. Jonson and G. D. Mahan, Phys. Rev. B **21**, 4223 (1980).

⁵ U. Sivan and Y. Imry, Phys. Rev. B **33**, 551 (1986).

⁶ L. W. Molenkamp, H. van Houten, C. W. J. Beenakker, R. Ep-

penga, and C. T. Foxon, Phys. Rev. Lett. **65**, 1052 (1990).

⁷ N. J. Appleyard, J. T. Nicholls, M. Y. Simmons, W. R. Tribe, and M. Pepper, Phys. Rev. Lett. **81**, 3491 (1998).

⁸ G. Granger, J. P. Eisenstein, and J. L. Reno, Phys. Rev. Lett. **102**, 086803 (2009).

⁹ N. Read and D. Green, Phys. Rev. B **61**, 10267 (2000).

¹⁰ M. Büttiker, Phys. Rev. Lett. **57**, 1761 (1986).

- ¹¹ S. Datta, *Electronic Transport in Mesoscopic Systems* (Cambridge University Press, Cambridge, 1995).
- ¹² G. E. Blonder, M. Tinkham, and T. M. Klapwijk, *Phys. Rev. B* **25**, 4515 (1982).
- ¹³ N. R. Claughton and C. J. Lambert, *Phys. Rev. B* **53**, 6605 (1996).
- ¹⁴ M. P. Anantram and S. Datta, *Phys. Rev. B* **53**, 16390 (1996).
- ¹⁵ We should point out that a voltage across the interface between a normal metal and a superconductor in response to the temperature difference between the two regions had been observed in the past^{23,24}. However, it had not been established whether the Mott formula is applicable to such a setup.
- ¹⁶ C.-Y. Hou, K. Shtengel, G. Refael, and P. M. Goldbart, *New Journal of Physics* **14**, 105005 (2012).
- ¹⁷ S. M. Reimann and M. Manninen, *Rev. Mod. Phys.* **74**, 1283 (2002).
- ¹⁸ K. T. Law, P. A. Lee, and T. K. Ng, *Phys. Rev. Lett.* **103**, 237001 (2009).
- ¹⁹ Chiral Majorana edge modes considered here should not be confused with Majorana *zero* modes; in our case these modes are formed out of the gapless states within the superconducting gap. Strictly speaking, these Majorana modes are not even energy eigenstates as they mix $\pm E$ states.
- ²⁰ N. W. Ashcroft and N. D. Mermin, *Solid State Physics* (Harcourt College Publishers, New York, 1976).
- ²¹ J. Li, G. Fleury, and M. Büttiker, *Phys. Rev. B* **85**, 125440 (2012).
- ²² L. Fu and C. L. Kane, *Phys. Rev. Lett.* **102**, 216403 (2009).
- ²³ D. Harlingen, *Journal of Low Temperature Physics* **44**, 163 (1981).
- ²⁴ J. R. Waldram and S. J. Battersby, *J. Low Temp. Phys.* **86**, 1 (1992).